Journal of Computer-Aided Molecular Design, 10 (1996) 284–292
ESCOM

J-CAMD 353

A proposed common spatial pharmacophore and the corresponding active conformations of some peptide leukotriene receptor antagonists

V. Hariprasad and Vithal M. Kulkarni*

Pharmaceutical Division, Department of Chemical Technology, University of Bombay, Matunga, Bombay 400019, India

Received 5 October 1995
Accepted 15 April 1996

Keywords: Conformational analysis; Pharmacophore; 3D QSAR; pLT receptor antagonists

Summary

Molecular modeling studies were carried out by a combined use of conformational analysis and 3D-QSAR methods to identify molecular features common to a series of hydroxyacetophenone (HAP) and non-hydroxyacetophenone (non-HAP) peptide leukotriene (pLT) receptor antagonists. In attempts to develop a ligand-binding model for the pLT receptor, the Apex-3D program was used to identify biophoric structural patterns that are common to 13 diverse sets of compounds showing different levels of biological activity. A systematic conformational analysis was carried out to obtain sterically accessible conformations for these flexible compounds. Apex-3D was then utilized to propose common biophoric regions based on the selection of one of several conformations (MOPAC-minimized AM1) from each compound's data set that best fits the biophoric pattern and the resulting superimposition with all the other data-set compounds. Apex-3D identified three common biophoric features important for activity: one as the hydroxyl, acetyl, carbonyl and carboxyl groups, which mimic the acid-binding region of an agonist, the other as the hydrogen-bond donating site, and the third part is represented by a plane in which lipophilic aromatic groups align. The structure–activity relationships were then assessed by using the 3D-QSAR model. A common biophore model is proposed from the Apex-3D analysis which may be useful in designing new pLT antagonists. Molecular volumes and electrostatic potential similarities were also calculated in order to obtain the important structural requirements for the activity.

Introduction

Enzymic oxidation of arachidonic acid via the lipoxygenase pathway gives rise to a group of biologically important mediators: the peptide leukotrienes (pLTs) C, D, and E (LTC_4, LTD_4, and LTE_4) have been identified as important components of slow-reacting substances of anaphylaxis (SRS-A) [1,2]. These leukotrienes have been chemically synthesized [3] and their biological effects have been investigated [4]. The pLTs are reported as powerful inflammatory agents that induce edema formation, bronchoconstriction and airway mucus secretion [5], and they also play important roles in bronchial asthma [6], ischemia [7], shock [8], and other pathological events [9]. In addition the pLTs stimulate the proliferation of various cell types [10]. The identification of leukotriene receptors has spurred an interest in the development of pLT antagonists as potential therapeutic agents for the treatment of allergic asthma and other immediate hypersensitivity diseases [11,12].

In an effort to characterize pLT binding sites and to develop common structural features among pLT receptor ligands, the structure–activity relationships (SAR) of numerous inhibitors have been studied [13–17]. On the basis of SAR studies, the structural similarities between hydroxyacetophenone (HAP) and indole and indazole derivatives [18] that directly contribute to binding and selectivity for pLT receptors have been identified. The receptor model for pLTs has been proposed based on the natural agonist and on the SAR of pLTs and known receptor antagonists [19].

Since no structural information is available about the receptor active site, an indirect approach was adopted in attempts to understand the important interactions necessary for binding. This approach is referred to as receptor mapping or biophore (pharmacophore) identification. In

*To whom correspondence should be addressed.

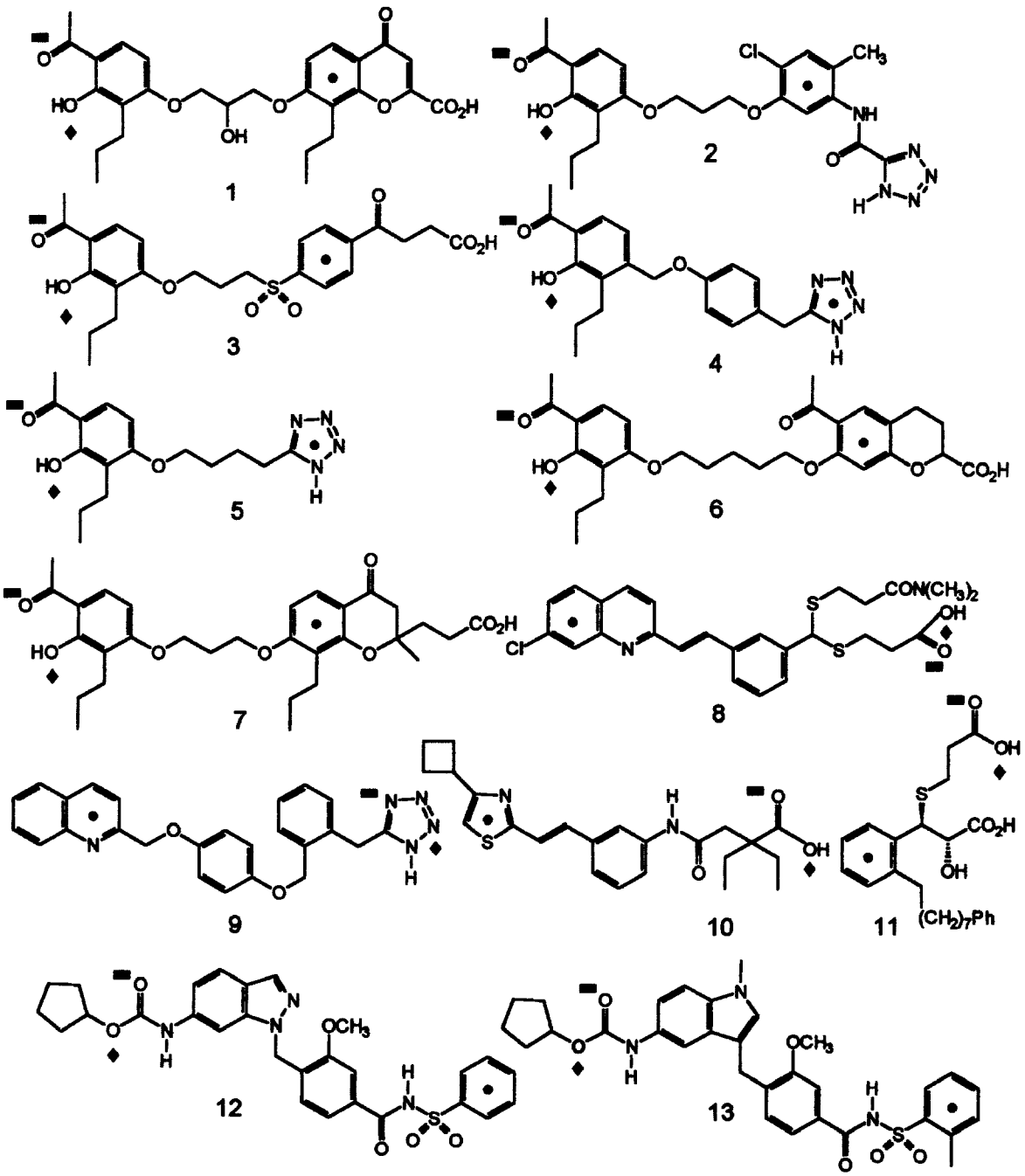

Fig. 1. Structures of 13 training set molecules of HAP (1–7) and non-HAP (8–13) pLT receptor antagonists. The atoms labeled ■, ♦, ● are the main structural features (biophores) identified by Apex-3D.

the present work, using Apex-3D (Biosym Technologies, Inc., San Diego, CA), a common biophore for 13 synthetically derived pLT receptor antagonists (Fig. 1) taken from the literature [20] as hydroxyacetophenone (HAP) (1–7) and non-hydroxyacetophone (non-HAP) (8–13) antagonists has been identified.

In search for a common relative spatial disposition of molecular features considered relevant for biological activity, the molecules are characterized by conformational analysis. Sterically accessible conformations of each compound are evaluated and compared in search for the common spatial pharmacophore that constitutes the active conformation which was used as the biophore model for the pLT receptor. On the basis of statistically significant biophoric features identified by Apex-3D, a common spatial biophore has been proposed for these ligands. The atoms considered in the biophoric definition in each compound are labeled in Fig. 1 and their main interatomic distances between the biophoric descriptors are shown in Fig. 2a. A 3D-QSAR (three-dimensional quantitative structure–activity relationship) method [21,22] was used to construct a valid 3D geometrical model for pLT re-

TABLE 1
CONFORMATIONAL DATA, ENERGY OF THE GLOBAL MINIMA AND BIOLOGICAL ACTIVITY OF HAP AND NON-HAPs FOR THE pLT RECEPTOR

Compound	Conformers[a]	Energy[b] (ΔE)	pKB[c]
1 FPL-55712	63	3.55	6.7
2 CGP-35949	33	6.93	7.4
3 L-648,051	45	3.75	7.3
4 LY163443	3	5.46	7.5
5 LY171883	6	5.29	6.9
6 Ro-23-3544	103	3.38	6.6
7 SC-39070	16	1.33	8.2
8 MK-571	34	4.74	9.3
9 RG 12525	24	4.55	8.4
10 Ro-24-5913	55	4.99	9.3
11 SKF 104353	117	2.10	8.6
12 ICI 198615	57	5.01	10.1
13 IC 204219	69	5.45	9.5

[a] Within 10 kcal mol^{-1} above that of the lowest energy conformation found.
[b] Energy difference between the Apex-3D conformer and the lowest energy conformer.
[c] pKB = –log kB.

ceptor antagonists. The 3D geometrical requirements for each molecule were described by using interatomic distances between the four descriptors that are present in all the training sets of molecules which were considered most significant for interaction with the pLT receptor. Steric and electronic properties were calculated and used in the evaluation of similarity between compounds upon identification of active conformations of each ligand.

Computational methods

The molecular structures of HAPs and non-HAPs were drawn in 2D and converted to 3D using the *Sketch* and *Converter* functionality in INSIGHT II [23] and then MOPAC-minimized (AM1) to provide reasonable standard geometry. In order to include the electrostatic term, atom-centered charges were calculated [24], and the quantum-mechanical molecular electrostatic potential (MEP) was generated by using the semiempirical molecular orbital AM1 [25] method as implemented in the MOPAC [26] program. These charges were used in the conformational search procedure.

A systematic conformational search in the *Search/Compare* module located sterically accessible conformations for these structures using a rotation increment of 30° for all the torsional angles. These conformational results were verified by means of the molecular mechanics method using the Conjugate Gradient algorithm of the DISCOVER 2.9.5 program (Biosym Technologies [27]). The list of allowed conformations was too large; therefore the lowest energy conformers for each compound having potential energies below 10 kcal mol^{-1} of the current global minimum were saved. New charges were assigned when the proposed active conformations were selected upon completion of the conformational search, as MEP-derived charges are slightly dependent on molecular conformation [28].

Apex-3D was then used for automated pharmacophore identification and 3D-QSAR model building. Statistically significant biophores and their active conformations from Apex-3D analysis were used in the calculation of molecular volumes. Volumes were visualized through Boolean grid representations of the superimposed molecules generated using the *volume/create* option of INSIGHT II.

The electrostatic potential similarities [29] between each pair of molecules, as well as the overall similarity, were calculated using the *overlap/electrostatic* option of the *Search/Compare module* on the basis of charges calculated by AM1, and the potential similarities were analyzed by optimizing the fit. All calculations were performed on a Silicon Graphics INDY R4400 workstation.

Results and Discussion

The aim of present computer-aided molecular modeling (CAMM) studies has been the development of a common spatial pharmacophore model for the diverse set of compounds that have the binding affinity for the pLT receptor. From conformational analysis, the lowest energy conformer of each molecule was considered as the active conformer and compared with the low-energy conformers of all the other molecules in order to obtain a common alignment (optimization of superimposition) model to accommodate all the molecules. The Apex-3D program was then used for the automated pharmacophore identification and 3D-QSAR model building to construct an active model for the pLT receptor, which may be useful as a template for the design of new pLT receptor antagonists.

TABLE 2
APEX-3D MODEL RELIABILITY EVALUATION

No. of compounds	Model	RMSA	RMSP	R^2	Chance	Match
12	I	0.44	0.48	0.91	0.04	0.36
11	II	0.52	0.60	0.85	0.03	0.31
11	III	0.53	0.58	0.83	0.01	0.24
11	IV	0.51	0.54	0.84	0.02	0.22
13	V	0.48	0.51	0.86	0.06	0.19

TABLE 3
APEX-3D STATISTICAL PARAMETERS FOR pKB DATA AT THE pLT SITES FOR HAP AND NON-HAP LIGANDS

	3D-QSAR models				
	I	II	III	IV	V
r^2 non-cross[a]	0.907	0.853	0.831	0.842	0.860
PRESS[b]	1.516	2.140	2.489	2.327	2.284
S[c]	0.435	0.517	0.526	0.509	0.478
F-test	25.891	23.126	44.183	47.886	30.702
n[d]	12	11	11	11	13
Contributions[e]					
hydrophobic	3.41	1.47	−2.07	−1.81	−2.32
steric	0.96	−1.89	−0.97	−2.09	1.05

[a] r^2 represents the non-cross-validated square of the correlation coefficient between experimental and approximated activity.
[b] PRESS represents the prediction sum of squares for residuals.
[c] S represents RMSA (root-mean-square error of activity approximation).
[d] n represents the number of compounds in the training set.
[e] Average model variable contributions.

Conformational analysis

In order to identify statistically significant biophores for these flexible compounds that require only a representative selection that spans conformational space, a set of conformers was generated by the systematic conformational searching method using molecular mechanics CVFF (consistent valence force field) calculations as described in the Computational Methods section. The low-energy bioactive conformers were identified that present the pharmacophore. Due to the high flexibility of the compounds, the number of conformers generated was too large, a *set_energy_params* command was used to specify the maximum conformers to 100 and the molecular mechanics energy threshold to 10 kcal mol^{-1} to reduce the number of conformers for finding conformers that are energetically most stable. The resulting conformers in the current global minimum were saved. To filter out conformers that will not add new information on biophore geometry and resultant superpositioning of these flexible compounds, Apex-3D was then utilized for internal conformer clustrization in which the sample of conformers for each compound is divided into a number of clusters. After the conformer clustering, the lowest energy of each cluster is selected as representative of that cluster and exported to Apex-3D, which is available as a module in INSIGHT II 2.3.5 software for automated biophore identification and 3D-QSAR model building.

Apex-3D analysis

Apex-3D uses a logico-structural approach [30] to identify molecular features common to a set of diverse chemical structures. Advanced statistical techniques and 3D pattern-matching algorithms are used to assign probabilities for the identified biophores that are causing biological activity for these ligands. These biophores are composed of various descriptor centers. Calculations with Apex-3D were performed on these sets of compounds. Apex-3D was asked to consider the following properties

TABLE 4
STRUCTURE–ACTIVITY DATA OF THE EXPERIMENTAL AND PREDICTED pKBs FROM APEX-3D ANALYSIS

Compound	3D-QSAR models					Experimental
	I	II	III	IV	V	
1	6.70	7.06	7.30	7.33	7.32	6.70
2	–	7.84	7.19	7.22	7.20	7.40
3	7.46	6.50	7.20	7.23	7.22	7.30
4	8.67	7.56	7.17	7.20	7.18	7.50
5	6.19	7.27	7.27	7.30	7.28	6.90
6	6.85	7.34	7.32	7.35	7.33	6.60
7	7.86	7.27	7.05	7.09	7.07	8.20
8	9.13	–	–	8.99	9.63	9.30
9	8.75	7.74	–	–	8.60	8.40
10	8.22	9.74	9.28	–	9.63	9.30
11	8.82	–	9.48	9.15	8.40	8.60
12	10.44	9.26	9.54	10.40	9.37	10.1
13	9.34	9.90	9.22	8.95	9.57	9.5

for structure–activity relationships: hydrogen bonding sites, partial charges on heteroatoms, electron donor and acceptor indices and aromatic ring centroids. One of the statistically significant alignment models is identified and its pharmacophoric site points are shown in Fig. 2b. Apex-3D identified the following features important for activity that included all the training compounds (Table 1) superimposed on to four distinct pharmacophoric site points: an aromatic ring center, two atom-centered descriptors and a receptor associated hydrogen bond donor. These features agree very well with the SAR for this series of compounds. Initially, five models were selected

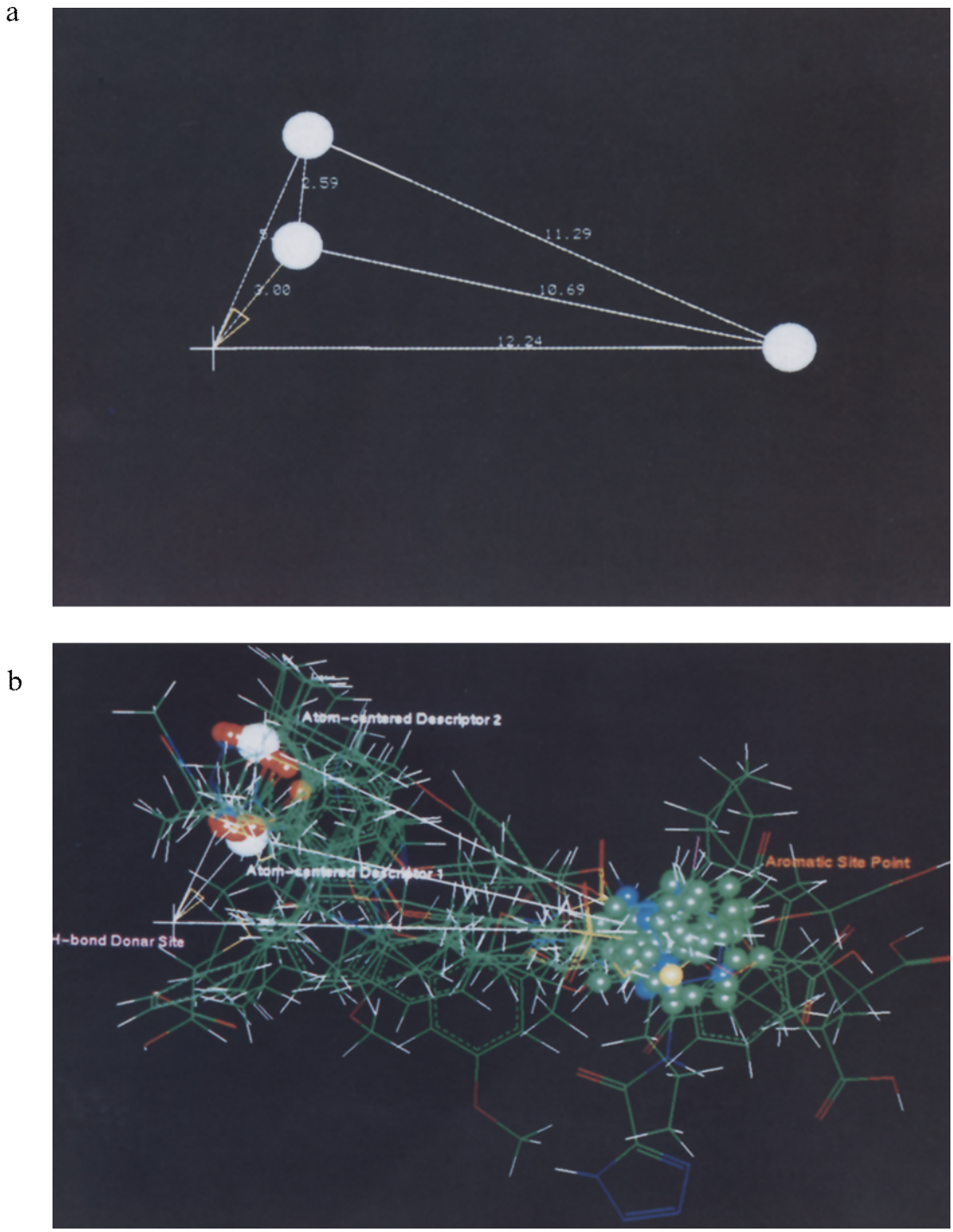

Fig. 2. (a) View of the biophore and the important descriptors considered in the biophore definition. The distance ranges are given in Å. (b) Optimization of superimposition (alignment) and biophoric site points of a statistically significant biophore model I identified by Apex-3D. White spheres denote atom-centered descriptors. The cone represents a hydrogen-bond donor, and the gold sphere a ring center.

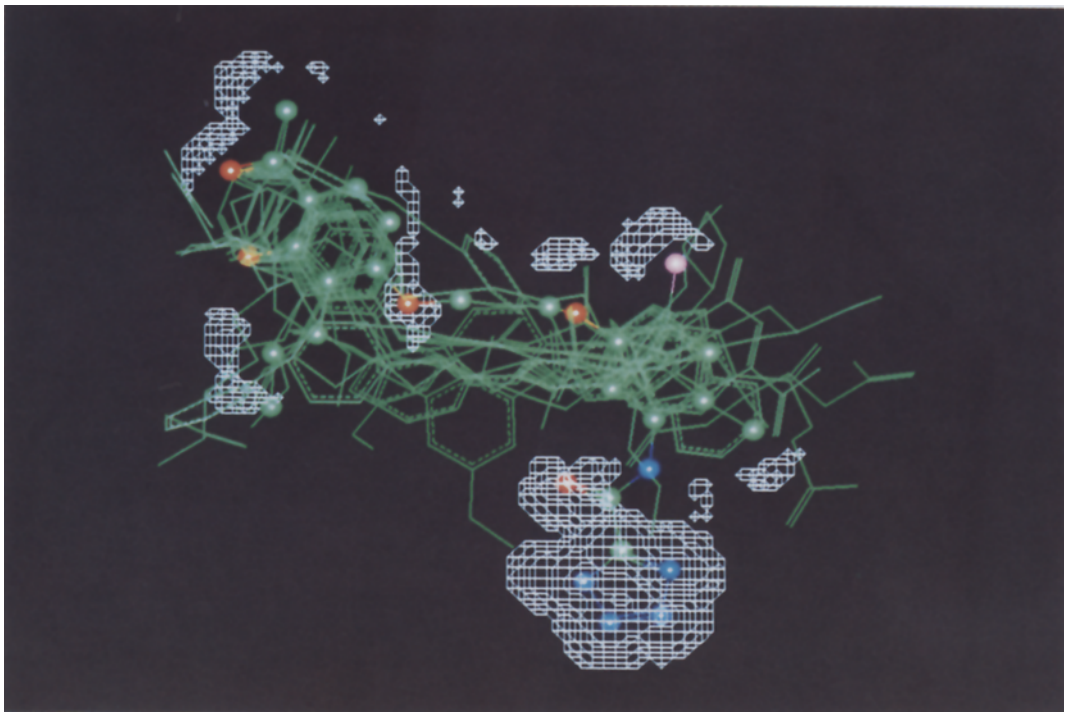

Fig. 3. The volume difference of compound **2** with **1**, **3–7** and **8–13**. There are many small discrete regions of volume difference, but the most significant difference is occupied by the tetrazole substituent.

with one model associated with each conformer of the training set. The selection of an appropriate model is based on the minimal deviation of the superimposed biophoric centers, the best possible fit of each of the superimposed ensembles, and the results obtained from 3D-QSAR analysis. A pharmacologically relevant model would be associated with an initial positive R^2 when considered in the training set. This hypothesis was used

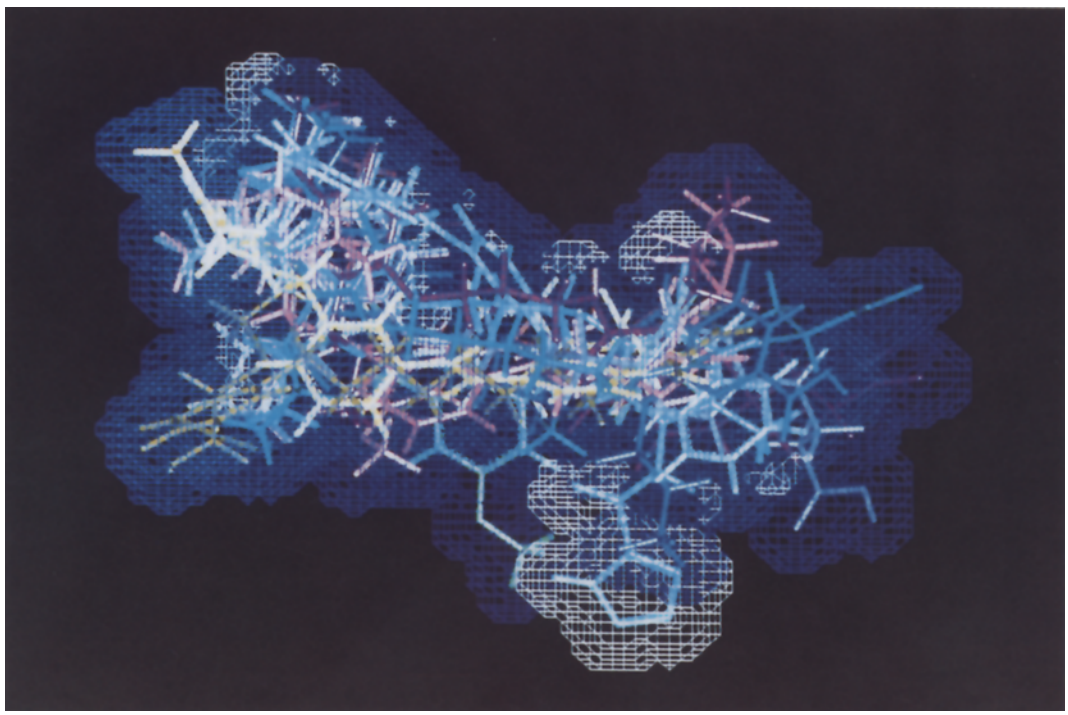

Fig. 4. Superimposition of HAPs and non-HAPs and their volume map, illustrating regions occupied by **1**, **3–7** and **8–13** compounds (blue) that are not shared by compound **2** (white).

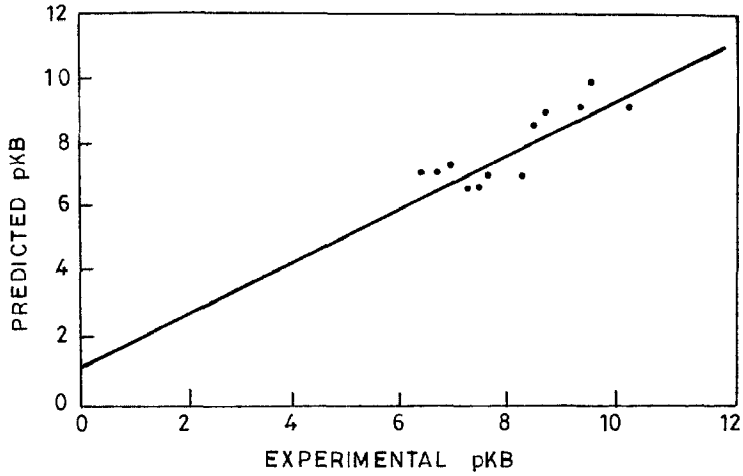

Fig. 5. Plot of experimental versus predicted pKB values for the set of 12 pLT antagonists belonging to model I.

as an initial screening process whereby each model was subjected for 3D-QSAR reliability checking and subsequently to a leave-one-out cross-validation (cv) analysis (13 compounds). The results of initial analysis are listed in Table 2. During the selection of significant biophore model compounds having a large difference in leave-one-out predictions, the RMSA (root-mean-square error of activity approximation) and RMSP (root-mean-square error of activity prediction calculated using cross-validation) that are overfitted by the multiple regression and are poorly predicted were not included in the training set. The probability of chance correlations greater than 0.1 were excluded from further consideration. Biophores that have representative compounds with a high match were further used in 3D-QSAR model building.

The statistically most significant model I having 12 compounds in the training set was considered. None of the structural features of the compounds (**1**, **3–13**) extended beyond the steric region, whereas structure **2** not aligned in this model was eliminated. This was further explained by calculating the volume difference between the compounds **1**, **3–13** and compound **2** as shown in Fig. 3. This illustrates that compound **2** protrudes from the union volume, presumably due to some steric clash in the active site. A superimposition of compound **2** with compounds **1**, **3–13** within the ligand-excluded space (Fig. 4) illustrates that the binding region would require specific volume or may have an auxiliary binding region that can accommodate large substituents such as those associated with compound **2**. Electrostatic potential similarity calculations were also performed and are discussed in the Volumes section.

3D QSAR

The basic statistical tool for 3D-QSAR model building in Apex-3D is the stepwise regression algorithm [21]. This algorithm selects multiple regression equations by deleting and adding variables using the F-test criteria. The regression analysis was performed on the training set of compounds of five models obtained from initial model building. The results of statistically significant biophore models of regression analysis applied on the training set data are reported in Table 2. The stepwise F-test performed on the PRESS (prediction sum of squares) values with no cross-validation justifies model I as the most appropriate pharmacophore alignment. The accuracy of the non-cross-validated predictions was assessed by observing the resulting prediction error values. The results of 3D-QSAR studies are presented in Table 3. The difference between observed and predicted pKB [31] (pKB = –log kB for leukotriene antagonists on LTD_4 contraction in guinea pig trachea) values is listed in Table 4 and plotted in Fig. 5. In order to visualize the information contents of the 3D-QSAR model, biophore pseudoatoms were generated and a reliable model for 3D-QSAR coefficients and their associated standard deviations was calculated. Initial analysis based on model I yielded a correlation with a non-cross-validated r^2 of 0.91 ($F = 25.891$) using 12 training set compounds. The RMSA is 0.44 and the RMSP is 0.48, which implies good predictive ability (the coefficient of correlation is 0.952) for the test set of pLT antagonists with an average mean-square variance of 0.190. We found that the following relationship, analyzed in terms of hydrophobicity (log P) and steric factor, shows significant correlation of the efficacy of these compounds as pLT antagonists:

$$\text{activity} = 7.89\ \text{pKB} + 0.314\ (\text{hydrophobic site 1}) - 1.886\ (\text{steric site 2})$$

$$n = 12,\ r^2 = 0.91,\ \text{RMSA} = 0.44,\ \text{RMSP} = 0.48$$

Thus log P, by itself, is a good descriptor of the activity of these compounds. By virtue of its association with transport and distribution (pharmacokinetic) in biological fluids and tissues log P is deemed important.

Model II yielded poor correlation ($r^2 = 0.853$ with 11 compounds) and prediction RMSE (0.603). This is possibly indicative of poor molecular alignment. The secondary hydrophobicity, steric and pi-SUM site points were added to the model to improve the statistics. A new model was generated with three variables with a sensitivity of 7. By doing this the explained variance was 85%, the RMSA was 0.52, and the prediction error was 0.603. The conventional statistical results ($r^2 = 0.853$) and the predictive ability of this model for the 11 test compounds were not affected by the changes in the addition of secondary sites. Model III produced a statistically significant coefficient of correlation (0.911); the probability of chance correlation was very large (0.10) and expressed a highest average analysis variance of 0.227. Even though the rest of the statistics for this equation are good, it is not reliable for the activity prediction and is not a good model.

Models IV and V produced a correlation with a cross-validated prediction RMSE of 0.554, 0.507 using 11 and 13 compounds, respectively, with $r^2 = 0.842$, 0.860 with an average analysis variance of 0.259 and 0.228. This is much worse than previous results; also there is a more than 20% chance that this is a fortuitous correlation. Based on these results, the final 3D-QSAR model I was selected and was found to have the best predictability with about a 3% chance of being fortuitous. The incorporation of parameters such as frontier molecular orbital HOMO and LUMO energies failed to enhance the correlation coefficients derived for these charged compounds.

Based on the maximal deviation of the superimposed biophoric centers and on the elimination of one or two compounds with large residuals, the statistics showed an improved correlation in certain Apex-3D training set models from the several cross-validated analyses. Model V showed a significant increase in the r^2 value to a maximum of 0.893 when compound **2** was excluded from the training set, which showed the maximal deviation from alignment. This was further rationalized by examining the volumes.

Volumes

Apex-D has placed all the compounds in the biophore model that are important for activity, yet are actually different in biological efficacy. This is rationalized by examining the volume difference. Molecular volumes of the compounds used in the final Apex-3D analysis were visualized through Boolean grid representations of the superimposed molecules. The total volume of the 13 training set molecules and their volume difference with compound **2**, in which the tetrazole group protrudes from the union volume of a set of compounds, were calculated and are shown in Figs. 3 and 4. Visualization of the volumes that contribute to the binding affinities of the pLTs indicates specific regions for high affinity to pLTs. Although there are many small discrete regions of difference volume, the most significant is occupied by the tetrazole group of compound **2**. It appears that pLT cannot accommodate large substituents such as present in compound **2**. Superimposition of compound **2** with other pLT antagonists indicates that the binding region would require specific volume in the receptor pocket.

The electrostatic potential similarity calculation and optimization have been performed for the comparative evaluation of 13 pLT receptor ligands using the Hodgkin index as discussed by Good et al. [29] for multiple molecules:

$$SF = \frac{2}{M(M-1)} \sum_{a=1}^{M-1} \sum_{b=a+1}^{M} SF(a,b)$$

where M is the number of molecules. The electrostatic potential of molecules is dependent on the atomic charges and distances. The electrostatic potential similarity between each pair of molecules as well as the overall similarity show maximal dissimilarity, which is about 0.485. There is an improved electrostatic potential fitting of 0.489 when compound **2** is not considered. Essentially no additional information is obtained relative to volume representations. Thus both geometrical and electronic properties must be taken into consideration to rationalize their efficacy.

Conclusions

The Apex-3D methodology has been applied in 13 chemically diverse test sets of HAP and non-HAPs binding to the pLTs. The resulting 3D-QSAR model derived from a training set of 12 compounds and the elimination of one compound from the initial Apex-3D analysis show a significant correlation of hydrophobic and steric factors with biological activity. The predictions agree well with the experimental values. This rationalizes the binding affinity in terms of hydrophobic and steric properties. The Apex-3D biophore model reveals regions in 3D space around these ligands and provides a hypothetical picture of the main chemical features responsible for pKB variations. Presently, the output from these analyses in the form of the Apex-3D biophore model is being used in the design of novel pLT inhibitors. Using the selected 3D-QSAR model I, we have identified potential lead compounds which show high predicted potencies. The results of these rational design efforts will be reported elsewhere.

Acknowledgements

The authors thank the University Grants Commission (UGC), New Delhi, for financial support under its DSA project. The authors also thank Dr. Reddy's Research Foundation, Hyderabad, India.

References

1 Samuelsson, B., Science, 220 (1983) 568.
2 Lewis, R.A., Austen, K.F. and Soberman, R.J., New Engl. J. Med., 323 (1990) 645.
3 Corey, E.J., Clark, D.A., Goto, G., Marfat, A., Mioskowaski, C., Samuelsson, B. and Hammarstrom, S., J. Am. Chem. Soc., 102 (1980) 1436.
4 Lewis, R.A., Drazen, J.M., Rigueiredo, J.C., Corey, E.J. and Austen, K.F., Int. J. Immunopharmacol., 4 (1982) 85.
5 Samuelsson, B., Dahlen, S.E., Lindgren, J.A., Rouzer, C.A. and Serhan, C.N., Science, 237 (1987) 1171.
6 Lewis, R.A., Chest (Suppl.), 87 (1985) 55.
7 Lefer, A.M., Biochem. Pharmacol., 35 (1986) 123.
8 Piper, D.J., In Buckle, D.R. and Smith, H. (Eds.) Development of Anti-Asthma Drugs, Butterworths, London, 1984, p. 174.
9 Lewis, R.A., Austen, K.F. and Soberman, R.J., New Engl. J. Med., 323 (1990) 645.
10 Stenke, L., Mansour, M., Reizenstein, P. and Lindgren, J.A., Blood, 80 (1993) 352.
11 Shaw, A., Annu. Rep. Med. Chem., 25 (1990) 61.
12 Nakai, H., Konno, M., Kosuge, S., Sakuyama, S., Toda, M., Arai, Y., Obata, T., Katsube, N., Miyamoto, T., Okegawa, T. and Kawasaki, A., J. Med. Chem., 31 (1988) 84.
13 Dillard, R.D., Carr, P.E., Kalaus, D.M., Haisch, K.D., Rinkema, L.E. and Fleisch, J.H., J. Med. Chem., 30 (1987) 911.
14 Matassa, V.G., Maduskuie, T.P., Shapiro Jr., H.S., Hesp, B., Snyder, D.W., Aharony, D., Krell, R.P. and Keith, R.A., J. Med. Chem., 33 (1990) 1781.
15 Gapinski, D.M., Roman, C.R., Richardson, L.E. and Fleisch, J.M., J. Med. Chem., 31 (1988) 172.
16 May, D.W.P., Newton, J.F., Torphy, J.J. and Gleason, J.G., Drugs Future, 15 (1990) 240.
17 Snyder, D.W., Giles, R.E., Keith, R.A., Yee, Y.K. and Krell, R.D., J. Pharmacol. Exp. Ther., 243 (1987) 548.
18 Brown, J.F., Yee, Y.K., Cronk, L.H., Hebbel, K.C., Krell, R.D. and Snyder, D.W., J. Med. Chem., 33 (1990) 1171.
19 Harper, R.W., Herron, D.K., Bollinger, N.G., Sawyer, J.S., Baldwin, R.F., Roman, C.R., Rinkema, L.E. and Fleisch, J.H., J. Med. Chem., 35 (1992) 1191.
20 Shaw, A. and Krell, R.D., J. Med. Chem., 34 (1991) 1235.
21 Golender, V. and Vorpagel, E., In Kubinyi, H. (Ed.) 3D QSAR in Drug Design: Theory, Methods and Applications, ESCOM, Leiden, 1993, pp. 137–149.
22 Van de Waterbeemd, H. (Ed.) Advanced Computer-Assisted Techniques in Drug Discovery, Vol. 3, VCH Publishers, New York, NY, 1994.
23 INSIGHT II (v. 2.3.5) 1995, Biosym Technologies, Inc., 9685 Scranton Road, San Diego, CA 92121, U.S.A.
24 Ferenczy, G.G., Reynolds, C.A. and Richards, W.G., J. Comput. Chem., 11 (1990) 159.
25 Dewar, M.J.S., Zoebiach, E.G., Healy, E.F. and Stewart, J.J.P., J. Am. Chem. Soc., 107 (1985) 3902.
26 Stewart, J.J.P., MOPAC: A general molecular orbital package (v. 6.0), QCPE #455.
27 Biosym Technologies, Inc., San Diego, CA.
28 Reynolds, C.A., Essex, J.W. and Richards, W.G., J. Am. Chem. Soc., 114 (1992) 9075.
29 Good, A.C., Hodgkin, E.E. and Richards, W.G., J. Chem. Inf. Comput. Sci., 32 (1989) 3.
30 Myers, R.H., Classical and Modern Regression with Application, PWS-KENT Publishing Company, 1990.
31 Snyder, D.W., Giles, R.E., Keith, R.A., Yee, Y.K. and Krell, R.D., J. Pharmacol. Exp. Ther., 243 (1987) 548.